ROXAS: a new spectral code for isolated neutron star gravitational wave signal.

Gaël Servignat

servignat@apc.in2p3.fr
Work carried in LUTH

GdR Ondes Gravitationnelles: Réunion du groupe de travail Formes d'ondes
June 28, 2024

Table of Contents

Table of Contents

Context

- Core collapse supernovae and binary merger simulations in General Relativity (GR) have gone under tremendous progress during the last ∼25 years.
- Shibata and Uryu: first 3D binary neutron star (NS) merger simulation [Shibata and Uryū, 2000].
- Valencia formulation [Banyuls et al., 1997; Font, 2008]: conservative formulation of GR-hydro equations.
- Development of high-resolution shock capturing (HSRC) methods.
- Numerical Relativity (NR) simulation of compact binary mergers: waveforms of inspiral + merger + ringdown.
- Next two decades: post-O5 runs of LIGO-Virgo-Kagra + Einstein Telescope & Cosmic Explorer, sensitivity increased in the kHz band.

Hydrodynamics

- Most hydrodynamical codes rely on conserved variables [Banyuls et al., 1997; Font, 2008].
- Different discretisation: finite volume [Cipolletta et al., 2021], Smooth Particle Hydrodynamics [Rosswog and Diener, 2021], spectral methods [Hébert et al., 2018].
- Allows the treatment of shocks.
- Inspiral + merger simulations possible.
- Conserved $\leftrightarrow$ physical (*primitive*) variables computationally expensive.
- Only $\sim$500 merger simulations in two decades: too few for a parametric study.

Goal

Writing a full-GR, full non-linear neutron star evolution code for post-merger phase.

- Final goal: run simulations of a post-merger hypermassive neutron star with 3-parameter equations of state (EoS), perform a parametric study by varying the EoS.
- Test beds in spherical symmetry with barotropic EoS.
- Axisymmetric and non-axisymmetric frequency extraction with barotropic EoS.
- Waveform extraction (gravitational waves signal).

We consider a perfect fluid of baryons carried by a timelike unitary 4-velocity u^ν:

$$T^{\mu\nu} = (e+p)u^\nu u^\mu + pg^{\mu\nu}$$

with e the total internal energy, p the fluid pressure, $g^{\mu\nu}$ the metric which is decomposed in the 3+1 formalism:

$$g_{\mu\nu}\mathrm{d}x^\mu \mathrm{d}x^\nu := -N^2\mathrm{d}t^2 + \gamma_{ij}(\mathrm{d}x^i + \beta^i \mathrm{d}t)(\mathrm{d}x^j + \beta^j \mathrm{d}t)$$

with N the lapse function, β^i the shift vector and γ_{ij} the 3-metric.

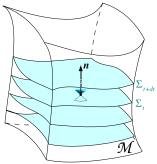

Figure: 3+1 foliation in spacelike hypersurfaces

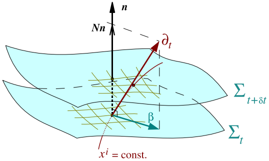

Figure: Illustration of the lapse and the shift

Framework
Primitive variables

Physical variables are called "primitive" variables:

- e the energy density, p the pressure
- n_B the baryon number density
- m_B a baryon mass
- $H = \ln\left(\frac{e+p}{m_B n_B}\right)$ the log-enthalpy
- U_i the Eulerian velocity field
- v_i the coordinate velocity field
- c_s the sound speed

Table of Contents

Conservative variables

The variables $D = m_B n_B \Gamma^2$, $S_j = (e+p)\Gamma^2 U_j$ and $\tau = (e+p)\Gamma^2 - p$, with $\Gamma = (1 - U_i U^i)^{-1/2}$ the Lorentz factor, are conserved in the sense that $\mathbf{u} = (D, S_j, \tau)$ obeys an equation that looks like

$$\partial_t \mathbf{u} + \mathrm{div}(F(\mathbf{u})) = \mathrm{source}$$

but the knowledge of e, p, U_i is compulsory to solve Einstein equations to compute the metric. **Recovery procedures are needed to recover the primitive variables in multiple steps of NR codes and account for a significant part of the computation:**

- Solving for the metric.
- Solving for the Riemann problems in each grid cell at each time step.

New set of equations using primitive variables [Servignat et al., 2023]

From the principles of stress-energy and baryon number conservation:

$$\nabla_\mu (n_B u^\mu) = 0, \ \nabla_\mu T^{\mu\nu} = 0,$$

the following holds for a barotropic, non-reactive perfect fluid with K_{ij} the extrinsic curvature tensor:

$$\begin{aligned}
\partial_t U_i = & -v^j D_j U_i - D_i N - \frac{N}{\Gamma^2}\left(D_i H - \frac{\Gamma^2(1-c_s^2)}{\Gamma^2 - c_s^2(\Gamma^2-1)} U_i U^j D_j H\right) \\
& + U_j D_i \beta^j + U_i U^j D_j N \\
& + \frac{N c_s^2}{\Gamma^2 - c_s^2(\Gamma^2-1)} U_i D_j U^j + \frac{N\Gamma^2(c_s^2-1)}{\Gamma^2 - c_s^2(\Gamma^2-1)} U_i U^j U^l K_{jl} \\
\partial_t H = & -v^i D_i H - c_s^2 N \frac{\Gamma^2}{\Gamma^2 - c_s^2(\Gamma^2-1)}\left[U^i U^j K_{ij} - \frac{U^i}{\Gamma^2} D_i H + D_i U^i\right]
\end{aligned}$$

This new set of equations is **covariant** within the 3+1 formalism.
e, p, c_s are recovered in a single call to the EoS **(no iteration)**.

New set of equations using primitive variables [Servignat et al., 2023]

From the principles of stress-energy and baryon number conservation:

$$\nabla_\mu (n_B u^\mu) = 0, \ \nabla_\mu T^{\mu\nu} = 0,$$

the following holds for a barotropic, non-reactive perfect fluid with K_{ij} the extrinsic curvature tensor:

$$\begin{aligned}
\partial_t U_i = &- v^j D_j U_i - D_i N - \frac{N}{\Gamma^2}\left(D_i H - \frac{\Gamma^2(1-c_s^2)}{\Gamma^2 - c_s^2(\Gamma^2-1)} U_i U^j D_j H \right) \\
&+ U_j D_i \beta^j + U_i U^j D_j N \\
&+ \frac{N c_s^2}{\Gamma^2 - c_s^2(\Gamma^2-1)} U_i D_j U^j + \frac{N\Gamma^2(c_s^2-1)}{\Gamma^2 - c_s^2(\Gamma^2-1)} U_i U^j U^l K_{jl} \\
\partial_t H = &- v^i D_i H - c_s^2 N \frac{\Gamma^2}{\Gamma^2 - c_s^2(\Gamma^2-1)} \left[U^i U^j K_{ij} - \frac{U^i}{\Gamma^2} D_i H + D_i U^i \right]
\end{aligned}$$

This new set of equations is **covariant** within the 3+1 formalism.

e, p, c_s are recovered in a single call to the EoS **(no iteration)**.

Table of Contents

ROXAS: Numerical ingredients [Servignat & Novak, on arXiv very soon$^{\text{tm}}$!!]

ROXAS: **R**elativistic **O**scillations of non-a**X**isymmetric neutron st**A**r**S**

- Implementation based upon LORENE[a] (spectral methods).
- Two distinct grids (see next slide):
  1. Metric grid: spherical domains with nucleus, shells, CED.
  2. Hydro grid: one nucleus + shells.
- Hydro grid adapted to the surface of the star: deformed domains.
- Multi-domain matching.
- Filters.
- Well-balanced formulation of the equations.

- EoS: polytrope ($p = \kappa n_B^{\gamma}$)
- Dirac gauge + Maximal slicing.
- Einstein equations : fully constrained formalism (Poisson-like PDEs).
- Conformal Flatness Condition (CFC) = approximation.
- Time evolution with Adams-Bashforth explicit scheme (finite differences).
- The hydro grid external border is comoving with the star's surface.

[a] https://lorene.obspm.fr

Deformed domains

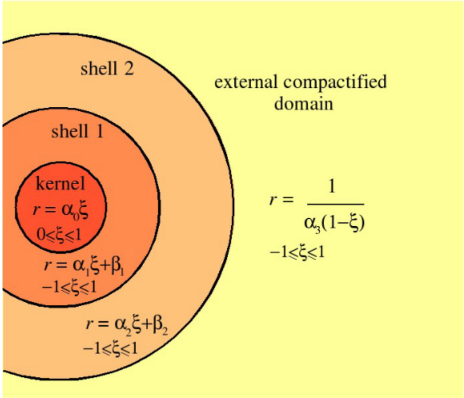

Figure: Metric grid: spherical numerical domains in LORENE.

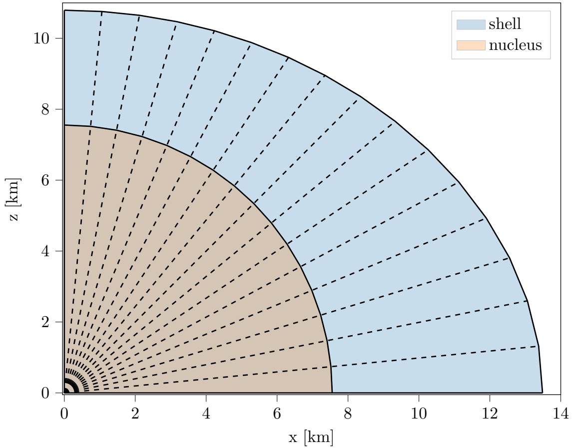

Figure: Hydro grid: deformed external domain (rotating star).

Validation of the code

Test beds in spherical symmetry [Servignat et al., 2023]:

- Migration test.
- Collapse to a black hole.
- Spherically symmetric oscillations + frequency extraction: Fourier transform of $R(t)$ (not shown here).

Non-spherically symmetric simulations:

- BU sequence: set of rigidly rotating polytropic NS + pseudo-polytropic representation of SLy4 EoS [Gulminelli and Raduta, 2015; Servignat et al., 2024].
- GW extraction with quadrupole formula (see next slides).
- Frequency extraction on $Y_{\ell m}$ decomposition of $R(t)$.

Validation of the relativistic code: migration test [Servignat et al., 2023]

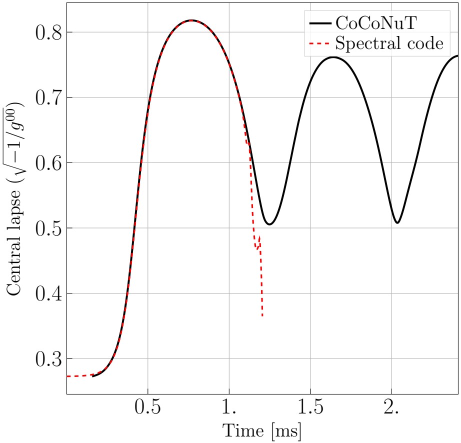

Figure: Central lapse.

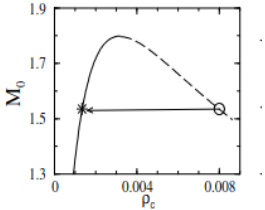

Figure: Migration test principle.

- Shock formation during the oscillations
- Gibbs phenomenon: the spectral code terminates.
- CoCoNuT: finite volume, high-resolution shock capturing techniques.
- 10s (spectral code) vs 6min (CoCoNuT).

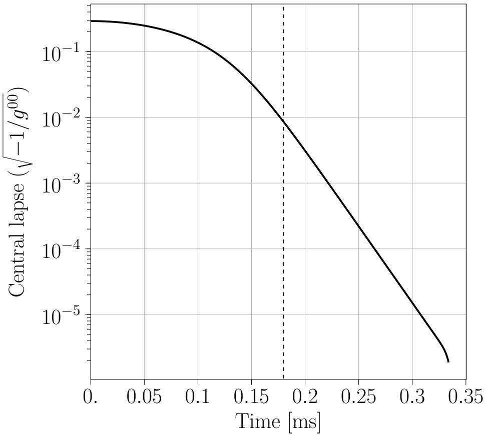

→ tests the strong gravity regime.

- Central lapse down to a few 10^{-6}.
- Freezing of the hydro quantities (maximal slicing).
- Apparent Horizon appearing around 0.18ms (dashed vertical line).

GW extraction: stress formula

- Quadrupole formula:

$$h_{ij}^{TT}(\boldsymbol{x},t) = \frac{2\mathcal{G}}{c^4 r} P_{ij}^{kl}(\boldsymbol{n}) \ddot{Q}_{kl}\left(t - \frac{r}{c}\right)$$

- Stress formula:

$$\ddot{I}_{ij} = \frac{\mathcal{G}}{c^4} \int\limits_{\mathbb{R}^3} \rho(\boldsymbol{x},t)(2v_i v_j - x_i \partial_j \Phi - x_j \partial_i \Phi)\, \mathrm{d}^3 x$$

- Plus/cross polarisation decomposition:

$$h_{ij}^{TT}(\boldsymbol{x},t) = \frac{1}{R}\left(A_+ \hat{\boldsymbol{e}}_+ + A_\times \hat{\boldsymbol{e}}_\times\right)$$

where

$$\hat{\boldsymbol{e}}_+ = \hat{\boldsymbol{e}}_\theta \otimes \hat{\boldsymbol{e}}_\theta - \hat{\boldsymbol{e}}_\varphi \otimes \hat{\boldsymbol{e}}_\varphi,$$

$$\hat{\boldsymbol{e}}_\times = \hat{\boldsymbol{e}}_\theta \otimes \hat{\boldsymbol{e}}_\varphi + \hat{\boldsymbol{e}}_\varphi \otimes \hat{\boldsymbol{e}}_\theta.$$

- Expression of A_+ and $A_\times$:

$$A_+^e = \ddot{I}_{zz} - \ddot{I}_{yy},\; A_\times^e = -2\ddot{I}_{yz}.$$

GW extraction: stress formula, improvements

- Weight method [Dimmelmeier et al., 2002]. Φ_1 pure Newtonian gravitational potential:

$$\Delta\Phi_1 = 4\pi\mathcal{G}\rho.$$

Relativistic gravitational potential in the Newtonian limit (exact up to first PN order):

$$\Phi_2 = \frac{1}{2}\left(1 - \Psi^4\right).$$

Weighted potential:

$$\Phi_w = \frac{\Phi_1 + a\Phi_2}{1+a}, \; a = \frac{1}{2}.$$

- Relativistic density

$$\rho^* = \Psi^6\Gamma\rho$$

- Replacing Newtonian velocity field v_i with relativistic Eulerian velocity field U_i.
- Final formula:

$$A_+^e = \frac{2\mathcal{G}}{c^4}\int_{\mathbb{R}^3}\rho^*(\boldsymbol{x},t)\left(U_z^2 - U_y^2 + y\partial_y\Phi_w - z\partial_z\Phi_w\right)\,\mathrm{d}^3x,$$

Numerical oscillations

BU4 model: rigidly rotating polytrope, $f_{\rm rot} = 673\,\mathrm{Hz}$.

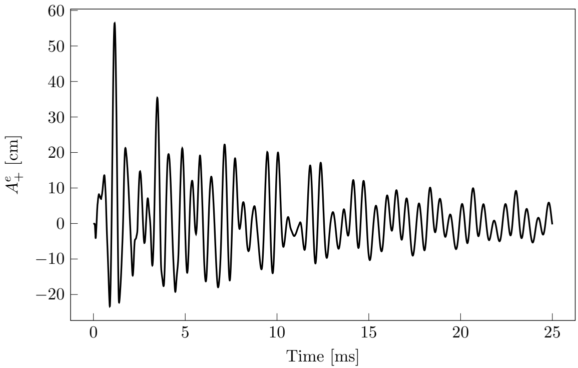

Figure: Waveform (BU4 model).

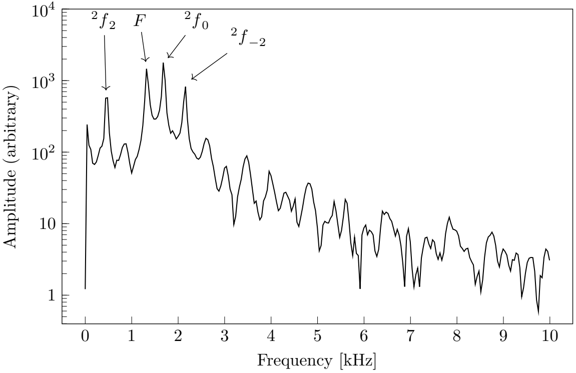

Figure: Spectrum (BU4 model).

Axisymmetric modes [Gaertig and Kokkotas, 2008; Dimmelmeier et al., 2006]

Model	f_{rot} [Hz]	M [$M_\odot$]	r_e [km]	$^2f_0$ [kHz]		Relative difference (%)	
				Cowling	CFC	Cowling	CFC
BU0	0	1.400	11.99	1.881	1.596	0.48	0.63
BU1	347	1.431	12.30	1.885	1.609	0.27	0.12
BU2	487	1.465	12.64	1.889	1.642	0.90	0.43
BU3	590	1.502	13.03	1.883	1.680	0.63	0.65
BU4	673	1.542	13.49	1.877	1.715	0.64	0.99
BU5	740	1.585	14.03	1.837	1.723	0.38	0.52
BU6	793	1.627	14.70	1.762	1.744	1.82	0.86
BU7	831	1.665	15.55	1.681	1.751	1.31	1.77
SLy4	191	1.361	9.34	2.400	1.964	×	×

Non-axisymmetric modes [Krüger et al., 2010; Krüger and Kokkotas, 2020]

Model	$f_{\rm rot}$ [Hz]	M [$M_\odot$]	r_e [km]	${}^2f_{-2}$ [kHz]		Relative difference (%)	
				Cowling	CFC	Cowling	CFC/GR
BU0	0	1.400	11.99	1.881	1.565	0.00	0.83
BU1	347	1.431	12.30	2.259	1.953	0.09	0.56
BU2	487	1.465	12.64	2.364	2.052	0.09	0.10
BU3	590	1.502	13.03	2.443	2.123	0.61	0.24
BU4	673	1.542	13.49	2.473	2.153	0.57	0.09
BU5	740	1.585	14.03	2.480	2.158	0.44	1.44
BU6	793	1.627	14.70	2.477	2.143	0.40	1.82
BU7	831	1.665	15.55	2.396	2.105	1.88	3.94
SLy4	191	1.361	9.34	2.640	2.185	×	3.7

Non-axisymmetric modes [Krüger et al., 2010; Krüger and Kokkotas, 2020]

Model	f_{rot} [Hz]	M [$M_\odot$]	r_e [km]	${}^2f_2$ [kHz]		Relative difference (%)	
				Cowling	CFC	Cowling	CFC/GR
BU0	0	1.400	11.99	1.881	1.565	0.00	0.83
BU1	347	1.431	12.30	1.367	1.080	0.51	0.09
BU2	487	1.465	12.64	1.121	0.840	0.98	0.48
BU3	590	1.502	13.03	0.918	0.640	0.09	0.63
BU4	673	1.542	13.49	0.721	0.451	1.66	1.11
BU5	740	1.585	14.03	0.520	0.280	2.69	4.64
BU6	793	1.627	14.70	0.348	0.130	2.01	12.3
BU7	831	1.665	15.55	0.163	×	11.0	×
SLy4	191	1.361	9.34	2.141	1.675	×	1.2

Table of Contents

Summary and outlook

- Development of a spectral code to evolve isolated neutron stars.
- New set of equations relying only on primitive variables.
- Non-barotropic, spherically symmetric oscillations studied in [Servignat et al., 2024].
- Extraction of non-axisymmetric mode frequencies with barotropic EoS (polytropes + one realistic EoS).
- GW signals extracted with quadrupole formula (+ improvements).

Summary and outlook

Assets:

- Very light code (3D simulations on laptop/office computer).
- Reasonable simulation time (still to be improved).
- No recovery procedure.
- Radius of the star followed by the grid.
- Very good frequency extraction (although CFC).
- Soon to be published/open source.

Drawbacks:

- In practice: no shock treatment.
- Spectral methods are unforgiving.
- Only oscillations/post-merger phase.

Outlook:

- Improve interpolation (high priority).
- Getting rid of CFC (low priority).
- Perform longer simulations.
- Implement differentially rotating profiles.

Thank you!

Figure: Roxas, the eponymous cat.

Bibliography I

Francesc Banyuls, Jose A. Font, Jose Ma. Ibanez, Jose Ma. Marti, and Juan A. Miralles. Numerical {3 + 1} General Relativistic Hydrodynamics: A Local Characteristic Approach. *Astrophysical Journal*, 476(1):221–231, February 1997. ISSN 0004-637X, 1538-4357. doi: 10.1086/303604. URL https://iopscience.iop.org/article/10.1086/303604.

F Cipolletta, J V Kalinani, E Giangrandi, B Giacomazzo, R Ciolfi, L Sala, and B Giudici. Spritz: general relativistic magnetohydrodynamics with neutrinos. *Class. Quantum Grav.*, 38 (8):085021, April 2021. ISSN 0264-9381, 1361-6382. doi: 10.1088/1361-6382/abebb7. URL https://iopscience.iop.org/article/10.1088/1361-6382/abebb7.

Isabel Cordero-Carrión, Pablo Cerdá-Durán, Harald Dimmelmeier, José Luis Jaramillo, Jérôme Novak, and Eric Gourgoulhon. Improved constrained scheme for the Einstein equations: An approach to the uniqueness issue. *Physical Review D*, 79(2):024017, January 2009. ISSN 1550-7998, 1550-2368. doi: 10.1103/PhysRevD.79.024017. URL https://link.aps.org/doi/10.1103/PhysRevD.79.024017.

H. Dimmelmeier, J. A. Font, and E. Müller. Relativistic simulations of rotational core collapse II. Collapse dynamics and gravitational radiation. *Astronomy and Astrophysics*, 393: 523–542, October 2002. ISSN 0004-6361. doi: 10.1051/0004-6361:20021053. URL `https://ui.adsabs.harvard.edu/abs/2002A&A...393..523D`. ADS Bibcode: 2002A&A...393..523D.

Harald Dimmelmeier, Nikolaos Stergioulas, and José A. Font. Non-linear axisymmetric pulsations of rotating relativistic stars in the conformal flatness approximation. *Monthly Notices of the Royal Astronomical Society*, 368:1609–1630, June 2006. ISSN 0035-8711. doi: 10.1111/j.1365-2966.2006.10274.x. URL `https://ui.adsabs.harvard.edu/abs/2006MNRAS.368.1609D`. ADS Bibcode: 2006MNRAS.368.1609D.

Bibliography III

José A. Font. Numerical Hydrodynamics and Magnetohydrodynamics in General Relativity. *Living Reviews in Relativity*, 11:7, September 2008. doi: 10.12942/lrr-2008-7. URL `https://ui.adsabs.harvard.edu/abs/2008LRR....11....7F`. ADS Bibcode: 2008LRR....11....7F.

Erich Gaertig and Kostas D. Kokkotas. Oscillations of rapidly rotating relativistic stars. *Phys. Rev. D*, 78(6):064063, September 2008. ISSN 1550-7998, 1550-2368. doi: 10.1103/PhysRevD.78.064063. URL `https://link.aps.org/doi/10.1103/PhysRevD.78.064063`.

F. Gulminelli and Ad. R. Raduta. Unified treatment of subsaturation stellar matter at zero and finite temperature. *Phys. Rev. C*, 92(5):055803, November 2015. ISSN 0556-2813, 1089-490X. doi: 10.1103/PhysRevC.92.055803. URL `https://link.aps.org/doi/10.1103/PhysRevC.92.055803`.

Bibliography IV

François Hébert, Lawrence E. Kidder, and Saul A. Teukolsky. General-relativistic neutron star evolutions with the discontinuous Galerkin method. *Physical Review D*, 98(4):044041, August 2018. ISSN 2470-0010, 2470-0029. doi: 10.1103/PhysRevD.98.044041. URL `https://link.aps.org/doi/10.1103/PhysRevD.98.044041`.

Christian Krüger, Erich Gaertig, and Kostas D. Kokkotas. Oscillations and instabilities of fast and differentially rotating relativistic stars. *Phys. Rev. D*, 81(8):084019, April 2010. ISSN 1550-7998, 1550-2368. doi: 10.1103/PhysRevD.81.084019. URL `https://link.aps.org/doi/10.1103/PhysRevD.81.084019`.

Christian J. Krüger and Kostas D. Kokkotas. Dynamics of fast rotating neutron stars: An approach in the Hilbert gauge. *Phys. Rev. D*, 102(6):064026, September 2020. ISSN 2470-0010, 2470-0029. doi: 10.1103/PhysRevD.102.064026. URL `https://link.aps.org/doi/10.1103/PhysRevD.102.064026`.

Bibliography V

S. Rosswog and P. Diener. SPHINCS_bssn: a general relativistic smooth particle hydrodynamics code for dynamical spacetimes. *Classical and Quantum Gravity*, 38:115002, June 2021. ISSN 0264-9381. doi: 10.1088/1361-6382/abee65. URL `https://ui.adsabs.harvard.edu/abs/2021CQGra..38k5002R`. ADS Bibcode: 2021CQGra..38k5002R.

Gaël Servignat, Jérôme Novak, and Isabel Cordero-Carrión. A new formulation of general-relativistic hydrodynamic equations using primitive variables. *Classical and Quantum Gravity*, 40(10):105002, May 2023. doi: 10.1088/1361-6382/acc828.

Gaël Servignat, Philip J. Davis, Jérôme Novak, Micaela Oertel, and José A. Pons. One- and two-argument equation of state parametrizations with continuous sound speed for neutron star simulations. *Physical Review D*, 109(10):103022, May 2024. ISSN 2470-0010, 2470-0029. doi: 10.1103/PhysRevD.109.103022. URL `https://link.aps.org/doi/10.1103/PhysRevD.109.103022`.

Bibliography VI

Masaru Shibata and Kōji Uryū. Simulation of merging binary neutron stars in full general relativity: Γ=2 case. *Phys. Rev. D*, 61(6):064001, March 2000. doi: 10.1103/PhysRevD.61.064001.

Hydrodynamics

The variables $D = m_B n_B \Gamma^2$, $S_j = (e + p)\Gamma^2 U_j$ and $\tau = (e + p)\Gamma^2 - p$, with $\Gamma = (1 - U_i U^i)^{-1/2}$, are conserved in the sense that $\mathbf{u} = (D, S_j, \tau)$ obeys an equation that looks like

$$\boxed{\partial_t \mathbf{u} + \mathrm{div}(F(\mathbf{u})) = \mathrm{source}}.$$

This formulation allows to sharply resolve shocks, but the knowledge of e, p, U_i is compulsory to solve EINSTEIN equations to compute the metric.

Recovery procedures are needed to compute the primitive variables and account for a significant part of the computation:

- Solving for the metric.
- Solving for the Riemann problems in each grid cell at each time step (finite-volume).

Frequency extraction principle

- Frequency extraction: spectrum computed with FFT algorithm on $R(t)$ then peak extraction.

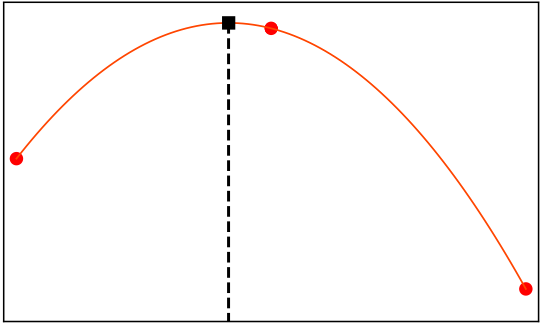

Figure: Frequency extraction principle.

Einstein equations

Lapse, shift, and 3-metric entirely determine the geometry of $\mathcal{M}$:

$$g_{\alpha\beta} = \begin{pmatrix} g_{00} & g_j \\ g_i & g_{ij} \end{pmatrix} = \begin{pmatrix} -N^2 + \beta_k \beta^k & \beta_j \\ \beta_i & \gamma_{ij} \end{pmatrix}$$

$\rightarrow$ The 3+1 formalism allows for a **natural separation of time and space**.

Definition of matter terms:

$$\begin{aligned} E &= T_{\mu\nu} n^\mu n^\nu \text{ the matter energy density,} \\ p_\alpha &= -T_{\mu\nu} n^\mu \gamma^\nu_\alpha \text{ the matter momentum density,} \\ S_{\alpha\beta} &= T_{\mu\nu} \gamma^\mu_\alpha \gamma^\nu_\beta \text{ the matter stress tensor,} \end{aligned}$$

and $S_t = S_{\alpha\beta}\gamma^{\alpha\beta}$ and $T = T_{\alpha\beta} g^{\alpha\beta}$.

Conformal decomposition

Let $\boldsymbol{f}$ be a flat metric of signature $(+,+,+)$. $(\mathcal{M}, \boldsymbol{g})$ is asymptotically flat i.e. $\gamma = \boldsymbol{f}$ at spatial infinity.

$$\boxed{\Psi = \left(\frac{\gamma}{f}\right)^{1/12}} \gamma = \det(\gamma_{ij}),\ f = \det(f_{ij})$$

Using

$$\tilde{\gamma}_{ij} = \Psi^{-4}\gamma_{ij}$$

The EINSTEIN equations become (using the CFC: $\tilde{\boldsymbol{\gamma}} = \boldsymbol{f}$):

$$\Delta\Psi = -2\pi\Psi^5\left[E + \frac{1}{16\pi}K_{ij}K^{ij}\right]$$

$$\Delta(N\Psi) = 2\pi N\Psi^5\left[E + 2S_t + \frac{7}{16\pi}K_{ij}K^{ij}\right]$$

$$\Delta\beta^i + \frac{1}{3}\bar{D}^i\bar{D}_j\beta^j = 16\pi N\Psi^4 p^i + 2\Psi^{10}K^{ij}\bar{D}_j\left(\frac{N}{\Psi^6}\right)$$

Conformal decomposition

Let $\boldsymbol{f}$ be a flat metric of signature $(+,+,+)$. $(\mathcal{M}, \boldsymbol{g})$ is asymptotically flat i.e. $\gamma = \boldsymbol{f}$ at spatial infinity.

$$\boxed{\Psi = \left(\frac{\gamma}{f}\right)^{1/12}} \gamma = \det(\gamma_{ij}),\ f = \det(f_{ij})$$

Using

$$\tilde{\gamma}_{ij} = \Psi^{-4}\gamma_{ij}$$

The Einstein equations become (using the CFC: $\tilde{\boldsymbol{\gamma}} = \boldsymbol{f}$):

$$\Delta\Psi = -2\pi\Psi^{5}\left[E + \frac{1}{16\pi}K_{ij}K^{ij}\right]$$

$$\Delta(N\Psi) = 2\pi N\Psi^5\left[E + 2S_t + \frac{7}{16\pi}K_{ij}K^{ij}\right]$$

$$\Delta\beta^i + \frac{1}{3}\bar{D}^i\bar{D}_j\beta^j = 16\pi N\Psi^4 p^i + 2\Psi^{10}K^{ij}\bar{D}_j\left(\frac{N}{\Psi^6}\right)$$

Uniqueness issue [Cordero-Carrión et al., 2009]

Additional conformal decomposition:

$$\hat{A}^{ij} = \Psi^{10} K^{ij}; \; \hat{A}^{ij} \approx \bar{D}^i X^j + \bar{D}^j X^i - \frac{2}{3} \bar{D}_k X^k f^{ij}.$$

Starred quantities:

$$E^* = \Psi^6 E, \; S_t^* = \Psi^6 S_t, \; p_j^* = \Psi^6 p_j.$$

Leads to:

$$\begin{aligned}
\Delta X^i + \frac{1}{3} \bar{D}^i \bar{D}_j X^j =& 8\pi f^{ij} p_j^*, \\
\Delta \ln \Psi =& -2\pi \Psi^{-2} E^* - \Psi^{-8} \frac{f_{il} f_{jm} \hat{A}^{lm} \hat{A}^{ij}}{8} - D_i \ln \Psi D^i \ln \Psi, \\
\Delta N =& 4\pi N \Psi^{-2} (E^* + S_t^*) + N \Psi^{-8} f_{il} f_{jm} \hat{A}^{lm} \hat{A}^{ij} - 2 D_i \ln \Psi D^i N, \\
\Delta \beta^i + \frac{1}{3} \bar{D}^i \bar{D}_j \beta^j =& \bar{D}_j (2N \Psi^{-6} \hat{A}^{ij}).
\end{aligned}$$

Uniqueness issue [Cordero-Carrión et al., 2009]

Additional conformal decomposition:

$$\hat{A}^{ij} = \Psi^{10} K^{ij};\ \hat{A}^{ij} \approx \bar{D}^i X^j + \bar{D}^j X^i - \frac{2}{3}\bar{D}_k X^k f^{ij}.$$

Starred quantities:

$$E^* = \Psi^6 E,\ S_t^* = \Psi^6 S_t,\ p_j^* = \Psi^6 p_j.$$

Leads to:

$$\begin{aligned}
\Delta X^i + \frac{1}{3}\bar{D}^i \bar{D}_j X^j &= 8\pi f^{ij} p_j^*, \\
\Delta \ln \Psi &= -2\pi \Psi^{-2} E^* - \Psi^{-8} \frac{f_{il} f_{jm} \hat{A}^{lm} \hat{A}^{ij}}{8} - D_i \ln \Psi D^i \ln \Psi, \\
\Delta N &= 4\pi N \Psi^{-2} (E^* + S_t^*) + N \Psi^{-8} f_{il} f_{jm} \hat{A}^{lm} \hat{A}^{ij} - 2 D_i \ln \Psi D^i N, \\
\Delta \beta^i + \frac{1}{3}\bar{D}^i \bar{D}_j \beta^j &= \bar{D}_j (2 N \Psi^{-6} \hat{A}^{ij}).
\end{aligned}$$

Validation of the relativistic code: frequency extraction [Servignat et al., 2023]

Table: Comparing the code and the literature.

	κ	γ	H_c $[c^2]$	M $[M_\odot]$	R [km]	Fund. [kHz]	1st ov. [kHz]	2nd ov. [kHz]
[?]	100	2	0.2279	1.4	14.15	1.450	3.958	5.935
This work	100	2	0.2279	1.401	14.16	1.442	3.954	5.915
Relative difference						0.6%	0.1%	0.3%
[?]	7.308	5/3	6.720×10^{-2}	$\times$	$\times$	0.824	1.94	2.86
This work	7.308	5/3	6.720×10^{-2}	0.4866	16.49	0.823	1.95	2.86
Relative difference						0.1%	0.5%	0.0%

Table: Cowling approximation (fixing spacetime to initial value).

	κ	γ	H_c $[c^2]$	M $[M_\odot]$	R [km]	Fund. [kHz]	1st ov. [kHz]	2nd ov. [kHz]
[?]	100	2	0.2279	1.4	14.15	2.696	4.534	6.346
This work	100	2	0.2279	1.401	14.16	2.685	4.548	6.339
Relative difference						0.4%	0.3%	0.1%